A COMPUTATIONAL COMPARISON OF ULTRASONICALLY INDUCED TISSUE HEATING BETWEEN CIRCULAR AND RECTANGULAR TRANSDUCER APERTURES

D.S. Ellis and W.D. O'Brien, Jr.

Department of Electrical and Computer Engineering
University of Illinois at Urbana-Champaign, Urbana, IL 61801

ABSTRACT

A comparison of theoretical tissue heating due to unscanned circular and rectangular focused ultrasound transducers has been performed. For comparison purposes, the same aperture area of π cm^2 and source power of 100 mW were used and the radius of the curvature for the rectangular aperture was the same as that for the circular case. The rectangular aperture was focused in the image plane and unfocused in the elevational direction. A homogenous-tissue model was used, and perfusion was taken into consideration. The temperature profile was generated by first calculating the relative field intensity values. These intensity values were then scaled to represent the same source power output for all constant-area transducer cases. Then the steady-state point-source solution of the bio-heat transfer equation was applied to determine the spatial thermal contribution for each field intensity value. By using superposition, the magnitude of the axial temperature was determined. For an aspect ratio of one, where the rectangular aperture is a square, the maximum temperature increase is approximately the same as that for the circular aperture. In general, the maximum temperature increase is greater for the circular source under these conditions.

INTRODUCTION

This study was set forth in order to examine the quantitative results of a method for determining the axial temperature increase in a homogenous medium when exposed to ultrasound. The previously published method and results were presented in the AIUM Bioeffects Report [1]. The AIUM report was limited to circular apertures. In this case, a more detailed model of tissue heating was developed and used to generate temperature profiles for both circular and rectangular aperture focused ultrasound transducers. This new method is required in order to evaluate the rectangular aperture case as the heated disc model is only valid for circularly symmetric beams.

The basis for comparison was presented in the AIUM Bioeffects Report in which a method for calculating the axial temperature increase in a homogenous medium was presented. The maximal temperature increase was determined by modeling the ultrasonic heat source as a superposition of heated discs. Each disc centered along the beam axis had a diameter equal to an effective beam width of a focused ultrasonic beam as deduced from work by Madsen et al [2].

The model reported herein for these calculations was based upon the point-source theory. The subsequent superposition of the temperature contributions of all of the point-sources in the medium was analyzed to generate the new temperature profiles. The comparison was extended by replacing the modeled circular aperture transducer with a rectangular aperture model and comparing the changes in the temperature profile. This method of generating temperature profiles could be extended for any geometrically modeled transducer and tissue model medium.

METHODS

In order to be able to establish the heated disc model as a reliable method, the results of AIUM [1] were reproduced. This was accomplished by mathematically modeling the effective beam width from the AIUM figure. The intensity and temperature calculations were based upon this modeled beam width. The presented point-source model was compared to these results.

In this study the comparison of focused transducers with circular and rectangular apertures was addressed. These transducers were modeled as a collection of point-sources evenly positioned on a geometric surface corresponding to either the circular or rectangular aperture, both of which were focused.

The circular aperture was modeled as a spherical segment with a radius equal to the radius of curvature (ROC) value (Fig 1). The transducer and the medium were mapped in Cartesian coordinates with the origin located at the centroid of the spherical segment. The z-axis (range) was perpendicular to the aperture with z = 0 defined on the transducer surface.

For the rectangular aperture, the same general approach was applied. In this case, a cylindrical segment was used (Fig 2) with the origin located at the center of the aperture. This geometry modeled the focusing in only one dimension. The aperture was focused in the image plane (x-z plane) and unfocused in the elevated plane (y-z plane). For the rectangular aperture, the determining factor in the dimensions of the aperture was the aspect ratio, that is, the ratio of the width of the transducer in the imaging plane, x_{width}, to that of the elevational direction, y_{width}, that is,

$$aspect\ ratio = \frac{x_{width}}{y_{width}} \qquad (1)$$

Because the surface area (projection of the aperture onto the x-y plane) of the transducer was held constant for both the circular and rectangular apertures, the aspect ratio determined the dimensions of the rectangular aperture.

1051-0117/91/0000-1133 $1.00 © 1991 IEEE

$$Area = \pi r^2 \ (circular) = x_{width} y_{width} \ (rectangular) \quad (2)$$

The transducers were modeled as a set of point-sources evenly positioned over the surface of the respective geometries. This was accomplished by defining a square grid in the x-y plane. At each point the mathematical representation of the respective geometry was used to determine the position of the point-source in the z-direction.

$$Sphere: \ x^2+y^2+(z-ROC)^2 = ROC^2, \quad -\frac{d}{2} \le x,y \le +\frac{d}{2} \quad (3)$$

$$Cylinder: \ x^2+(z-ROC)^2 = ROC^2, \quad (4)$$

$$-\frac{1}{2}x_{width} \le x \le \frac{1}{2}x_{width}, \ -\frac{1}{2}y_{width} \le y \le \frac{1}{2}y_{width} \quad (5)$$

where ROC is the radius of curvature of the transducer and d is the diameter of the circular aperture. The width of each grid point was $\lambda/6$, where λ is the ultrasonic wavelength in the medium. Thus, each point-source represented an area of $\lambda^2/36$.

For all of the computations, a homogenous tissue model was used. The quantities used to describe the medium are listed in Table 1. These values were the same as those presented in AIUM [1] for continuity of the comparison. The medium was mapped in Cartesian coordinates using the same set of axes and the same origin as described in the modeling of the transducers.

Table 1. Homogenous Tissue Model Quantities

c, the speed of sound	= 1540.0 m/sec
f, frequency	= 3.0 MHz
A, attenuation=absorption	= 0.15 Np/cm
ρ, density	= 0.001 kg/cm^3
L, perfusion length	= 1.18 cm
K, thermal conductivity coefficient	= 0.006 W/cm^2

Using the definition of the transducers and the homogenous medium already presented, the calculation of the relative intensity at each point in the medium was performed. The ultrasonic pressure at a point in the medium was determined by using the principle of superposition to add the contributions of each transducer point-source to the total complex pressure value. The first value to be calculated was the distance from the transducer point-source P_0 to the point in the medium P_1. This distance was calculated using the formula for distance between two points in space,

$$r=\sqrt{(x_1-x_0)^2+(y_1-y_0)^2+(z_1-z_0)^2} \quad (6)$$

where $P_0(x_0,y_0,z_0)$ represents the transducer surface point-source and $P_1(x_1,y_1,z_1)$ represents the point in the medium.

Once the distance is determined, the loss due to the attenuating medium was calculated. For each transducer point-source the pressure contribution was determined. The relative pressure at the point in the medium equals the contribution of all of the transducer point-sources,

$$p_{rel}(x_1,y_1,z_1)=\sum \frac{e^{-Ar}e^{jkr}}{r} \quad (7)$$

where A is the attenuation coefficient and k is the wave number ($2\pi/\lambda$).

After the contributions from all of the transducer surface point-sources were calculated, the complex relative pressure value was converted into a relative intensity value using the following equation.

$$I_{rel}(x_1,y_1,z_1)=p_{rel}(x_1,y_1,z_1)\cdot p^*_{rel}(x_1,y_1,z_1) \quad (8)$$

Thus, the relative intensity at any point in the medium could be obtained by providing the coordinates of the point in the medium and the geometric model of the transducer.

These relative intensity values were then scaled to reflect the source power level, W_0. Scaling was achieved by calculating the power for a fixed plane, perpendicular to the beam axis, which was the summation of the relative intensity values of each point in the plane perpendicular to the z-axis at a range z. This value was compared to the power, W(z), at that distance of the plane from the source, that is,

$$W(z)=W_0 e^{-2Az} \quad (9)$$

The scaling factor was the ratio of the power at z, W(z), to the computer power for the plane. Once the scaling factor was determined, each intensity value in the plane was scaled appropriately.

In order to evaluate and compare the computed beam profiles, the beam width was calculated. For each data plane perpendicular to the beam axis, the maximum intensity value was determined. These data were then scanned from the edge of the field toward the axis. The 10 dB value were defined as the first point encountered that was 1/10 of the maximum intensity value, respectively. Thus, the respective beam width was defined as twice the distance from the beam axis to the maximum intensity value in that plane.

In addition to the beam width, the spatial averaged intensity, or I_{SATA}, was computed. I_{SATA} is defined as,

$$I_{SATA}=\frac{W_{CS}}{AREA_{CS}} \quad (10)$$

where W_{CS} is the ultrasonic power within a given cross-section and $AREA_{CS}$ is the area of that cross-section. For the circular aperture, the cross-sectional area was defined as a circle with diameter equal to the calculated beam width. In the case of the rectangular apertures, two different cross-sections were used for comparison. One cross-sectional area that was used was a rectangle with the edge lengths equal to the beam width in the x and y directions. Another cross-section that was used was an ellipse with the axes of the ellipse defined as the beam width in the x and y directions.

From the intensity field the temperature increase along the z-axis can be calculated. A solution to the bio-heat transfer equation was presented by Nyborg [3]. This point-source solution provided a mathematical description of the steady-state temperature rise.

$$\Delta T=\frac{2C}{r}\exp\left(\frac{-r}{L}\right) \tag{11}$$

$$C=\frac{q_v\Delta v}{8\pi K}=\frac{(2\alpha I)\Delta v}{8\pi K} \tag{12}$$

where ΔT is the temperature rise above the ambient level, r is the distance from the point-source, L is the perfusion length, Δv is the volume of the point-source, K is the thermal conductivity coefficient, α is the absorption coefficient, and I is the ultrasonic intensity of the point-source. The temperature along the z-axis was formed by again using the superposition principle and summing the thermal contribution from every point-source in the medium to the points along the z-axis.

RESULTS

The technique for determining the thermal contribution as a superposition of point-sources was applied to several cases. In all cases, the quantities listed in Table 1 applied. The first case was that of a circular aperture focused transducer (Fig 1). This transducer had a diameter of 2 cm, an ROC of 10 cm, and a source power of 100 mW. The f number (ROC/diameter) for this case was 5. The 10 dB beam width of the ultrasonic field is presented in Fig 3. The resulting spatial averaged intensity is shown in Fig 4. The axial temperature profile is shown in Fig 5. The maximum temperature increase was 0.476°C and occurred at an axial distance of z = 1.07 cm from the transducer.

The second case was that of a rectangular aperture, where the aspect ratio was 1. The area of the aperture was π cm^2, the same as that for the circular case. The transducer had a radius of curvature of 10 cm in the imaging plane. Thus, the f number in the image plane for this case was 6.64. Fig 5 shows the temperature profile for this case.

DISCUSSION

In order to justify the results from the point-source temperature rise model, a direct comparison of the heated disc model [1] and the point-source model (Fig 5) was evaluated by comparing the results for the identical set of source and medium parameters. In Fig 6, the temperature profiles for both the heated disc model and point-source temperature rise model for the circular aperture are presented. The two sets of data are very similar in their maximum temperature increase and the axial distance at which that occurs. In the heated disc case, the maximum temperature increase is 0.492°C at z = 1.05 cm. The maximum temperature rise for the point-source model is 0.476°C at z = 1.07 cm. These two maximum temperature were considered to be equivalent when analyzing the differences in the model results.

However, the magnitude of the axial temperature increase is different for the two models near the focal region. This difference is explained by examining the effective beam widths for the two cases. AIUM [1] used as a function of range, the effective beam width near the focus as a sharp decrease followed by a linear increase as shown in Fig 3. The comparisons between the two models are strikingly similar except for the "less steep" change of the beam width around the focal region. This difference in the beam width data corresponds to a significant difference in the axial intensity profiles for the two models. Fig 4 shows the difference in the axial intensity (I_{SATA}) for the AIUM model and the calculated I_{SATA} from the calculated beam profile. The large difference in the intensity values in the focal region indicate that the I_{SATA} maximum near the focal region in AIUM [1] is actually a product of the modeling of the beam width and not result of the ultrasonic field. The comparison of the axial temperature profiles using the heated disc model and the calculated beam width as opposed to the effective beam width of AIUM [1] and the temperature profile generated for the point-source model (Fig 7) displays the validity of the point-source method for computing the axial temperature rise due to an ultrasonic field.

With the appropriateness of the point-source model justified, the use of this model for the rectangular aperture case followed. In determining the dimensions of the rectangular apertures, the surface area of both the circular and rectangular transducers are the same for comparison purposes. In the case of the circular aperture, the surface area is π cm^2. For the rectangular apertures, the cross-sectional area was equal to the circular aperture surface area of π cm^2 for each aspect ratio.

The important comparison to make is between the circular aperture case and the rectangular aperture case with an aspect ratio of 1. The temperature profiles exhibit the same characteristics, namely the singular maximum near 1 cm and the same general shape (Fig 5). The maximum temperature increase for the square aperture is lower than the circular aperture by 0.028°C or 5.9%. This small difference in the maximum temperature rise can be attributed to the difference in the distribution of the point-sources in that the distance from the four square corners were subjected to greater attenuation effects. The difference in the temperature increase can also be explained by the fact that for the circular aperture focusing is occurring in two dimensions while for the rectangular aperture there is only focusing in one dimension.

CONCLUSIONS

A new method for calculating the temperature increase in a homogenous tissue model has been presented. This method is not restricted to circular beams and therefore can be used to evaluate other geometries. By applying this model to exactly the same parameters as the heated disc model the following conclusions have been formed.

The maximum temperature increase for a circular aperture focused transducer is the same for both the heated disc and the point-source temperature rise models for the specified parameters. However, the heated disc model does not accurately predict the temperature rise near the focal region. This is due to the modeling of the beam width near the focal region.

The temperature rise for the square aperture (aspect ratio = 1) occurs at the same axial distance as for the circular aperture, but the maximum temperature rise for the square aperture is less than the maximum temperature of the circular aperture.

REFERENCES

[1] AIUM Bioeffects Committee, "Bioeffects considerations for the safety of diagnostic ultrasound," *J. Ultrasound Med.*, vol. 7, no. 9, pp. S8-S13, 1988.

[2] Madsen, E.L., M.M. Goodsitt and J. Zagzebski, "Continuous waves generated by focussed radiators," *J. Acoust. Soc. Amer.*, vol. 70, pp. 1508-1517, 1981.

[3] Nyborg, Wesley L., "Solutions of the bio-heat transfer equation," *Phys. Med. Biol.*, vol. 33, pp. 785-792, 1988.

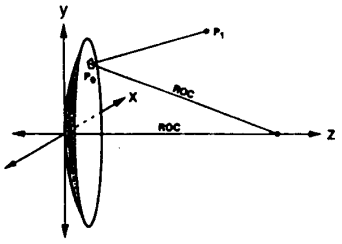

Fig 1. Focused circular transducer aperture model .

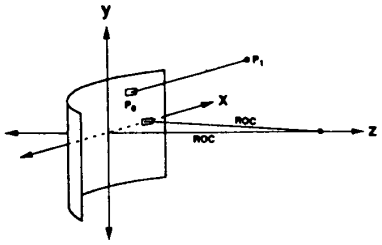

Fig 2. Focused rectangular transducer aperture model

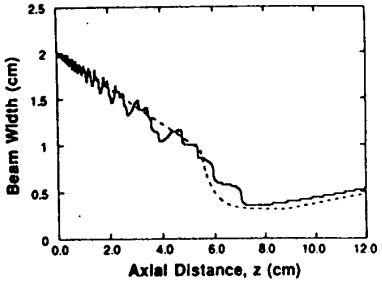

Fig 3. Beam width used for the heated disc model: AIUM (dashed), 10 dB (solid)

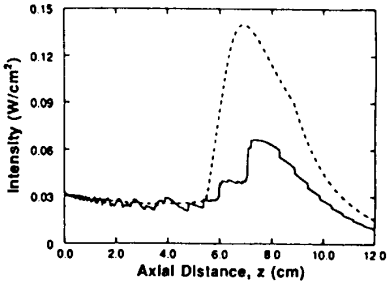

Fig 4. Spatial averaged intensity, I_{SATA}

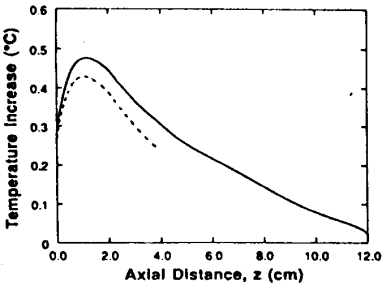

Fig 5. Axial temperature rise. Circular aperture (solid), diameter = 2 cm. Rectangular aperture (dashed), aspect ratio = 1. P_0 = 100 mW, ROC = 10 cm, and f = 3 MHz for both cases.

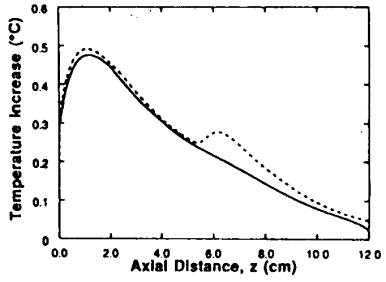

Fig 6. Comparison of axial temperature rises for the point-source (solid) and heated disc (dashed) methods.

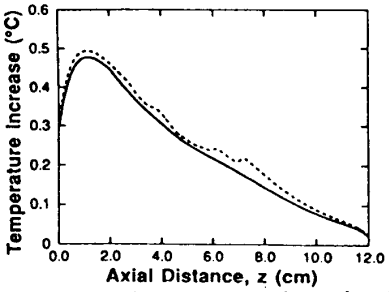

Fig 7. Comparison of axial temperature rises using the point-source method (solid) and the heated disc method (dashed) using the 10 dB beam width.